

Mechanical characteristics of multi-span concrete continuous girder oblique bridge based on ANSYS

Wan Ning*

Southwest Jiaotong University-Emei, Sichuan, China, 614202

Received 6 October 2014, www.cmnt.lv

Abstract

In order to adapt to environment and reduce the damage of construction for environment, the principle that environment adapts to construction is updated for bridge design, therefore lots special-shape bridges including oblique bridge emerge. However, there is no accurate and developed theory for computing the mechanical characteristics of oblique bridge. Generally, equivalent straight bridge is applied for computing. By performing finite element modelling, the internal force and displacement of oblique bridge and equivalent straight bridge with load were compared. The results showed that due to the special structure of oblique bridge, torque is generated under load, accompanying with coupling effect of bend-twist. Therefore, the mechanical characteristics analysis of straight bridge can not accurately explain that of oblique bridge.

Keywords: ANSYS, oblique bridge, computer simulations, finite element modelling

1 Introduction

Oblique bridge is a kind of special-shape bridges that different with straight bridge. Its normal line of bridge axis is not parallel to the support sides, between which the acute angle is called slope, which reflects the lean degree of the bridge. Benefited from high-grade highway, high-speed railway, urban three-dimensional traffic, etc. [1], oblique bridge develops continuously. With the development of economy, road network construction accelerates as well and new traffic lines are not always vertical to the existing lines and waterways in connection and crossing; considering the coordination with surrounding constructions and environment, the new traffic lines have to bring as little damage as possible to the environment; additionally, based on green building principle, the requirements for reducing water resistance ability of water piers and the navigation, and the change of design concept, the idea that traffic lines submit to bridges is not applicable any more. All these factors cause the existence of oblique bridge and its increasing proportion. To ensure quality of traffic lines, oblique bridges are mainly constructed in high-grade highways, such as urban three-dimensional traffic, expressway, and high-speed railway [2-

5]. Regarding mechanical characteristics, there are large differences between oblique bridge and straight one. Compared with straight bridge, oblique bridge generates torque and complex internal forces with bend-twist coupling under loads. There are many factors influencing the internal forces of oblique bridge, including supporting stiffness, stiffness ratio of bending and torsion, and the angle between bearing line and axis line, that is, the slope. At present, research on oblique bridge in China and abroad is in the initial stage and there is lack of perfect design theory and method. Moreover, there are no definite stipulations for mechanical characters, construction features, and construction points of oblique bridge in related specifications [6].

2 Static finite element analysis principle

Figure 1 shows a skew girder element in horizontal plane, and there are three degrees of freedom for the node [7-11]. Slope is the angle between the oblique section of end point and y-axis (symbol description: it is positive when y-axis clockwise turns to the oblique section; otherwise, it is negative).

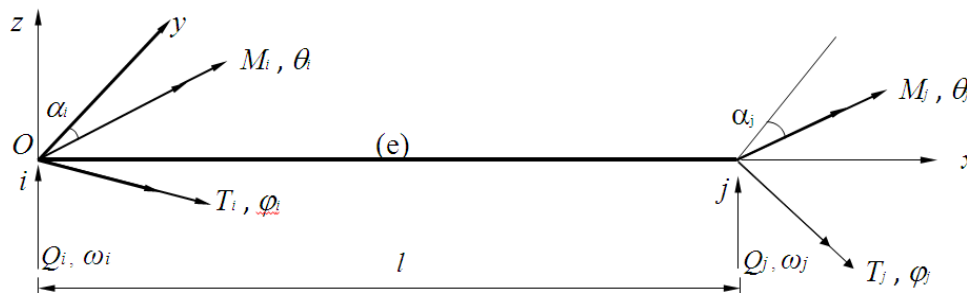


FIGURE 1 Skew girder element

*Corresponding author e-mail: ningwan@163.com

Suppose the i end of the element (e) is fixed and the j end is free, when there are forces Q_j, M_j and T_j on the j end, each component of the internal force of x section are:

$$\left. \begin{aligned} Q(x) &= -Q_j \\ M(x) &= Q_j(l-x) - M_j \cos \alpha_j + T_j \sin \alpha_j \\ T(x) &= -(M_j \cos \alpha_j + T_j \sin \alpha_j) \end{aligned} \right\} \quad (1)$$

The strain energy of the element is as follows without considering shear deformation:

$$\begin{bmatrix} \omega_j \\ \theta_j \\ \varphi_j \end{bmatrix} = \begin{bmatrix} \frac{l^3}{3EI} & -\frac{l^2 \cos \alpha_j}{2EI} & \frac{l^2 \sin \alpha_j}{2EI} \\ -\frac{l^2 \cos \alpha_j}{2EI} & \frac{l \cos^2 \alpha_j}{EI} + \frac{l \sin^2 \alpha_j}{GJ} & \frac{l \sin 2\alpha_j}{2GJ} - \frac{l \sin 2\alpha_j}{2EI} \\ \frac{l^2 \sin \alpha_j}{2EI} & \frac{l \sin 2\alpha_j}{2GJ} - \frac{l \sin 2\alpha_j}{2EI} & \frac{l \sin^2 \alpha_j}{EI} + \frac{l \cos^2 \alpha_j}{GJ} \end{bmatrix} \begin{bmatrix} Q_j \\ M_j \\ T_j \end{bmatrix} \quad (4)$$

That is:

$$\delta_j = D_{jj} F_j \quad (5)$$

The coefficient matrix D_{jj} is the flexibility matrix of the j end of the skew girder element. By performing inversion for the matrix, the stiffness matrix K_{jj} is:

$$K_{jj} = D_{jj}^{-1} \quad (6)$$

where D_{jj}^{-1} is stiffness ratio of bending and torsion, namely:

$$\lambda = \frac{EI}{GJ}$$

According to the equilibrium condition of the element, the relationship between force of i end and j end is:

$$F_i = H F_j \quad (7)$$

where H is stiffness transformation matrix.

The distal stiffness K_{ij} and proximal stiffness K_{ii} of i end of the element are:

$$K_{ij} = H K_{jj} \quad (8)$$

$$K_{ii} = H K_{jj} H^T \quad (9)$$

Therefore, the stiffness matrix of the skew girder element is:

$$K = \begin{bmatrix} H K_{jj} H^T & H K_{jj} \\ K_{jj} H^T & K_{jj} \end{bmatrix} \quad (10)$$

$$U = \frac{1}{2} \int_0^l \frac{M^2(x)}{EI} dx + \frac{1}{2} \int_0^l \frac{T^2(x)}{GJ} dx \quad (2)$$

According to Cass Tino theorem, we have:

$$\omega_j = \frac{\partial U}{\partial Q_j}, \theta_j = \frac{\partial U}{\partial M_j}, \varphi_j = \frac{\partial U}{\partial T_j} \quad (3)$$

Therefore, the relationship of the node displacement and the nodal force of j end of the element is expressed by

Suppose that the torsion angle function and the vertical displacement function of the element are cubic linear functions, the displacement function of the element is:

$$\delta(x) = N(x) \Delta \quad (11)$$

where $\delta(x)$ is the vector of the displacement function of the element.

$$\delta(x) = [\omega(x) \quad \theta(x) \quad \varphi(x)]^T \quad (12)$$

$$\Delta = [\omega_i \quad \theta_i \quad \varphi_i \quad \omega_j \quad \theta_j \quad \varphi_j]^T$$

Furthermore, the shape function of the element is calculated. After obtaining the shape function matrix, the equivalent nodal forces of each load are calculated based on energy principle.

3 Experimental case

The example in the research is a concrete double-line railway bridge with continuous rigid frame and three spans. The slope of the bridge is 45° , and large general finite element software ANSYS14.0 is used [12, 13]. The span of the equivalent straight bridge is the diagonal of the oblique bridge. No. shell181 plate element is applied in the construction of the upper structure of the bridge and the bridge pier model. Solid modelling is constructed by defining nodes first, through which establishing elements, and then building the overall model based on the elements (Figure 2). The rigid connection of pier and girder is simulated by coupling all degrees of freedom using nodes, and the pier bottom is restrained by consolidation. Static load simulation is conducted when two trains cross the bridge at the same time and produce maximum load.

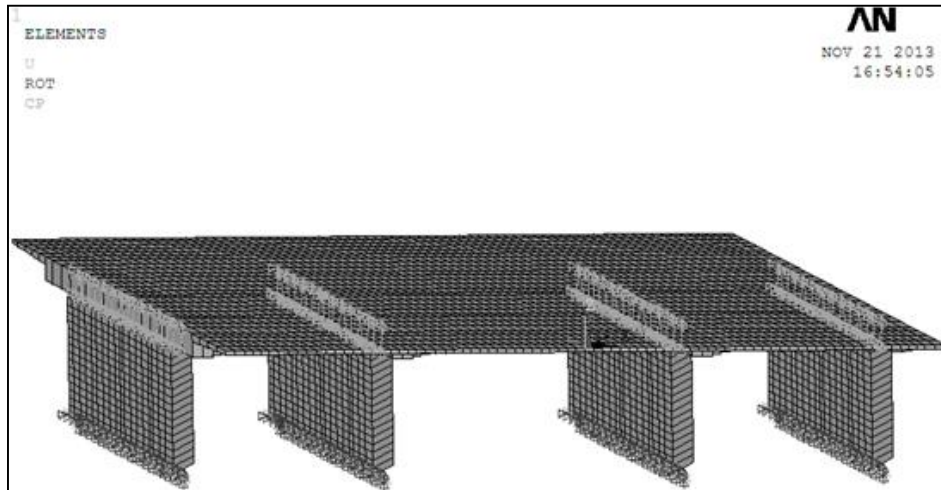


FIGURE 2 Whole oblique bridge model before the trains are loaded

3.1 DISPLACEMENT CALCULATION RESULTS

As there are lots nodes in the model, 21 key points in the oblique bridge and the straight bridge correspondingly are investigated to analyse their displacement, static force, and bending moment. The arrangement of the 21 points is demonstrated in Figure 3.

| | | | | | | |
|----|----|----|----|----|----|----|
| a1 | a2 | a3 | a4 | a5 | a6 | a7 |
| b1 | b2 | b3 | b4 | b5 | b6 | b7 |
| c1 | c2 | c3 | c4 | c5 | c6 | c7 |

FIGURE 3 Distribution of 21 key points in the research

The static force calculation for vertical displacement of the 21 points of the oblique bridge and the straight bridge is illustrated in Figure 4. By turning the calculation results around y-axis (along the transverse direction), the results are displayed in Figure 5.

Figure 4 shows the calculation results of vertical displacement. It indicates that under common medium-live load of bi-direction, the vertical displacement of the straight bridge is regular. The midpoints of each span are the maximum vertical displacements of each span (with maximum deflection). When the bridge is divided by the central point and there are equal loads along the both sides, the vertical displacement of the bridge is symmetric for the central point of the span. The vertical displacement at flange plate is close to 0 without obvious warping deformation. While under common medium-live load of bi-direction, the oblique bridge shows significant irregular vertical deformation. The calculation results display that the maximum vertical displacements of each span are also at the midpoints of each span. While, besides this, different with the straight bridge, distinct vertical deformations are observed at flange plate and the angular points (a1, c7) of the long diagonal, which causes irregular deformation of the whole bridge.

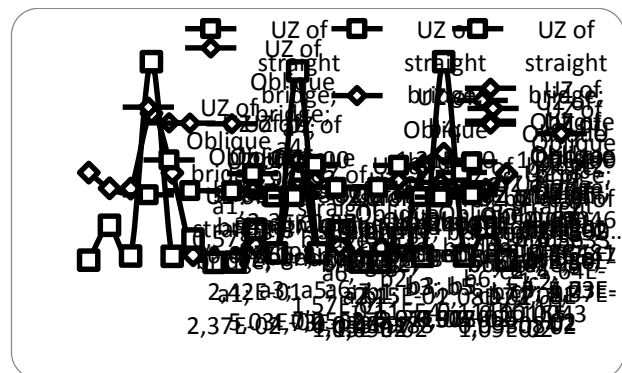


FIGURE 4 Calculation results of vertical displacements of the 21 points of oblique bridge and straight bridge (unit: mm)

The calculation results (Figure 5) demonstrates that the angular displacement of the straight bridge maintains dynamic equilibrium and fluctuates above and below zero alternately. The displacement is regular without apparent change. Meanwhile, the angular displacement of the oblique bridge is irregular and shows peak values. For examples, there are large angular displacements at the angular point, bridge pier, and the centres of spans at both sides. Therefore, there is obvious twist deformation of the surface of the oblique bridge.

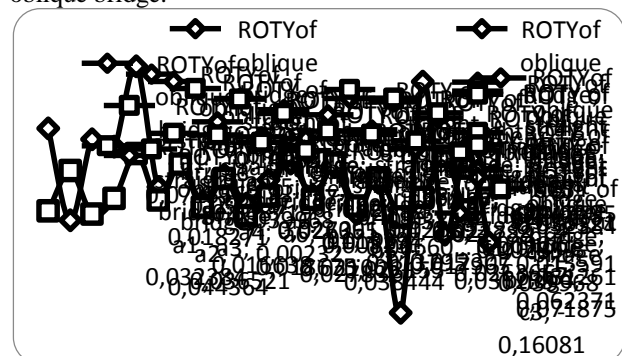


FIGURE 5 Angular displacements of straight bridge and oblique bridge by turning around y-axis (transverse direction) (unit: rad)

Merely specific points on each pier were analysed in the calculation of static internal forces, and the concrete positions of the points are demonstrated in the Figure below.

3.2 INTERNAL FORCE CALCULATION RESULTS

4 Conclusions and analysis

The static forces of the oblique bridge and the straight bridge are analysed and the comparison of calculation results of the axial force of the bridges is illustrated in Figure 6.

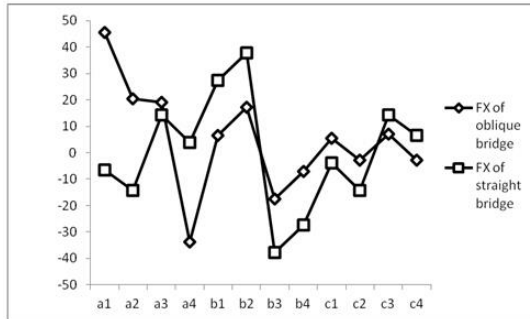


FIGURE 6 Calculation results of horizontal forces along the oblique bridge and the straight bridge (unit: kN)

It is observed in Figure 6 that among the selected points, the maximum axial horizontal force of the straight bridge is at the midpoint of the left central pier. The force is also positive. Maximum axial horizontal force difference (about 80 kN) is found between the midpoints of two central piers, where the directions of the two forces are opposite. For the oblique bridge, the variation of the axial horizontal force is mainly observed at two ends of the bridge, with a maximum difference of 90 kN around. Obviously, the mechanical character is different with that of the straight bridge.

Figure 7 shows that the maximum positive bending moment of the straight bridge is at the midpoint of the bridge surface and the maximum negative bending moment is at the left central pier. Considering the middle span, all the bending moments are large and positive and there is distinct variation of the bending moment along the axis. For the oblique bridge, the maximum positive bending moment is at point a3, which is near to the flange and the maximum negative bending moment is at the left bottom point a1. Meanwhile, the variation of bending moment along the axis is less than that of the straight bridge, with a maximum difference about 3 times. All these reveal that, for safety, it is better to calculate the bending moment along the axis using the data of straight bridge; while as the bending moments at side span and angular points of bridge surface are obviously different between the two bridges, the calculation of bending moments of oblique bridge using data of straight bridge can not ensure safety.

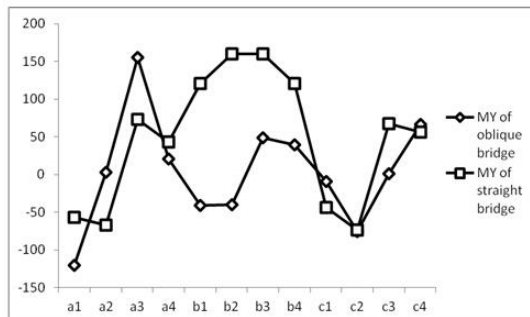


FIGURE 7 Bending moments of the oblique bridge and the straight bridge by turning around y-axis (unit: kN·m)

1) It is safe to calculate vertical displacement of oblique bridge using equivalent straight bridge at the midpoints of each span, where the vertical displacement of straight bridge are larger than that of oblique bridge. However, the vertical displacement of straight bridge is almost zero at flange and the oblique crossings of two ends; while oblique bridge generates coupling effect of bend-twist with load due to its special structure, and therefore leads to a larger internal force and large vertical displacements at the above positions. For example, obvious difference can be observed at the angular points (a1. c7), where there is no vertical displacement for straight bridge while about 0.6 mm of vertical displacement for oblique bridge. So, straight bridge cannot be applied in calculating vertical displacement of oblique bridge; otherwise, the safety of the oblique bridge cannot be guaranteed in usage.

2) The calculation of angular displacement by turning around y-axis shows that the angular displacement of straight bridge is stable without obvious variation; while owing to not completely symmetric structure, the oblique bridge generates torque under loads, accompanying with bend-twist coupling. This intensifies the local torsional deformation, for examples, the deformations at a5, c3, and c4. But the straight bridge is not influenced by the factor.

3) In the calculation of axial horizontal force, there is significant difference between the results of oblique bridge and the straight bridge. At some positions, the axial horizontal forces are in opposite directions, such as a1 and a4. There is about 50 Kn difference between the horizontal forces in the two computations, and the forces are in opposite indirections. Furthermore, the difference increases in dynamic calculation due to the movement of the loads. The inaccurate computation of horizontal force fails to accurately calculate and judge the stress and deformation of the bridge piers, and cannot provide valid data and reference for the design of lower structure. All these possibly cause transfinite deformation, even collapse of the bridge piers, therefore cannot guarantee the safety of the oblique bridge structure in usage.

4) Figure 7 demonstrates that, except several points are close to the straight bridge, the bending moments of oblique bridge around y-axis are significantly different with that of the straight bridge. This is clearly observed on the axis and angular points. On the axis, the maximum My difference reaches 200 Kn·m with opposite directions. When calculate bending moment using equivalent straight bridge, the tension and compression of girder and pier concrete of the oblique bridge cannot be accurately estimated. This probably causes that the tension of certain side of the concrete exceeds its tensile limit and therefore cracks. This inevitably threatens the safety of the bridge.

In summary, actual mechanical condition of oblique bridge cannot be accurately obtained in the computation of internal force and deformation using equivalent straight bridge, as the method fails to accurately consider or simulate the additional bending moment, coupling effect of bend-twist, non-uniform internal force and complex stress-strain

of the actual structure of oblique bridge. Presently, many scholars suggest that to improve the efficiency of the equivalent computing method by adding certain correction coefficient. However, with limited experience, specifications of each country have not provided accurate correction coefficients for each factor. Therefore, for safety, oblique bridges are generally designed with excessive bearing

and cost vast manpower and material resources. The method for computing mechanical characteristics of oblique bridge using equivalent straight is not scientific and applicable. Further research is needed to provide more accurate computing method or correction coefficients for each factor apart from finite element simulation.

References

- [1] Najafi F T, Nassar F E 1996 Comparison of high-speed rail and maglev systems *Journal of transportation engineering* **122**(4) 276-81
- [2] Zheng N, Aboudolas K, Geroliminis N 2013 Investigation of a city-scale three-dimensional Macroscopic Fundamental Diagram for bi-modal urban traffic *Proceedings of the IEEE Conference on Intelligent Transportation Systems ITSC 2013* 1029-34
- [3] Liu S, Wu Q 2009 Theory of "Compensating differential" for land expropriation in construction of expressway in China *Proceedings of the 2nd International Conference on Transportation Engineering ICTE 2009* 735-40
- [4] Deleted by CMNT Editor
- [5] Chen Y-S, Li B, Xiao R-M 2011 Transportation status of Chinese expressway network in 2010 *Jiaotong Yunshu Gongcheng Xuebao/Journal of Traffic and Transportation Engineering* **11**(6) 68-73 (in Chinese)
- [6] Nie Y, Qian C 2011 Constitutive relation of sulfate attacked concrete based on uniaxial loading *Advanced Materials Research* **168-170** 50-6
- [7] Wang Z-C, Ren W-X 2011 Dynamic analysis of prestressed concrete box-girder bridges by using the beam segment finite element method *International Journal of Structural Stability and Dynamics* **11**(2) 379-99
- [8] Deleted by CMNT Editor
- [9] Yang S-R, Zeng Q-Y 2011 Analysis of steel truss girder bridge vibrations by finite truss element method *Shenzhen Daxue Xuebao (Ligong Ban)/Journal of Shenzhen University Science and Engineering* **28**(3) 195-9 (in Chinese)
- [10] Zhang Y, Li L, Lin L, Sun X 2013 Beam-segment finite element analysis on shear lag effect of thin-walled box girder adopting additional deflection as generalized displacement *Tumu Gongcheng Xuebao/China Civil Engineering Journal* **46**(10) 100-7 (in Chinese)
- [11] Deleted by CMNT Editor
- [12] Zeng Y 2013 Three-dimensional rock slope stability analysis of the longjiang river bridge *Proceedings of the 2013 5th Conference on Measuring Technology and Mechatronics Automation ICMTMA 2013* 1260-3
- [13] Zhao M-H, Yin P-B, Zhang Y-J, Yang M-H 2013 The design and calculation method of pile-column bridge pier foundation in high and steep slope *Lixue/Engineering Mechanics* **30**(3) 106-11 (in Chinese)

Author



Ning Wan, born in November, 1978, Sichuan Province, P.R. China

Current position, grades: master at the School of Southwest Jiaotong University, China.

University studies: MSc in Electrical Engineering and Automation in 2008 at the University of Southwest, Jiaotong University in China.

Scientific interests: structural dynamics, earthquake bridge.

Publications: more than 5 papers.

Experience: teaching experience of 12 years, 3 scientific research projects.